Optimization of Color Filter Sensitivity Functions for Color Filter Array Based Image Acquisition

Manu Parmar and Stanley J. Reeves
Department of Electrical and Computer Engineering,
Auburn University, Auburn, AL

Abstract

Color filter array (CFA) based acquisition schemes allow for the acquisition of color images with a single optical sensor and are an integral part of most consumer-level digital camera pipelines. The CFA is a mosaic of color filters overlaid on the optical sensor such that only a single spectral band is acquired at a particular location. There is thus simultaneous sampling in the spectral and spatial dimensions. In this paper we propose a joint spatial-chromatic framework for the design of optimal spectral sensitivity functions for CFA filters. We design optimal sensitivity functions for the Bayer and seven alternate CFA arrangements and demonstrate the superior performance of CFAs with optimized color filters with respect to standard RGB and CMY filters in terms of both perceived quality and the s-CIELab metric.

Introduction

The optical sensing elements in digital image acquisition devices are typically charge coupled devices (CCD) or complementary metal oxide semiconductors (CMOS) [1]. Both of these sensor types are inherently monochromatic. The incident radiation at each pixel of a sensor array is integrated over a range of wavelengths (in which the device is sensitive) to give intensity values over the sensor-array. To acquire color images, filters that are sensitive in particular ranges in the visible spectrum are placed before the optical sensor-array in the imaging pipeline. The sensor-array output is then the image band corresponding to the color of the color filter. Since at least three color bands are required to display an image, at least three sensor-arrays with three different color filters are required to acquire a color image.

Such multi-sensor acquisition schemes have several drawbacks. The sensors and beam-splitters contribute substantially to the cost of the camera (sensors are $\sim 25\%$ of the cost of typical digital camera [2]). Also, since the color bands are acquired at different planes, a post-processing operation is required to correct for the associated misregistration. To avoid the cost and complexity of multi-sensor acquisition systems, most consumer-level digital color cameras only employ one optical sensor. The sensor is overlaid with a color filter array (CFA) such that only one color is sampled at each pixel location. The full-color image is reconstructed from the subsampled data in a later step commonly referred to as demosaicking. This spatial-chromatic sampling raises the following key issues: the design of the sampling pattern, the design of spectral transmittance functions for the colors filters, and finally, the design of the demosaicking algorithm.

The arrangement of color filters is designed based on a number of disparate requirements. Lukac and Plataniotis [3] provide a summary of CFA pattern design requirements and an analysis of the performance of various RGB-type CFA patterns. The most significant desirable feature of a CFA pattern, particularly for devices that have limited computational capabilities (cell-phone cameras, low-end digital still cameras, PDA cameras, etc.), is the ease of demosaicking. Regular, repeated CFA patterns work best to satisfy this requirement. Another useful feature of uniform CFA patterns is their relative immunity to optical and electrical cross-talk among pixels in the sensor array. Cross-talk or leakage between adjoining differently colored pixels can significantly alter the the effective spectral transmittance function of a pixel. Regular patterns ensure a measure of consistency in the transmittances of similarly colored pixels across a sensor-array. A drawback of regular arrays is that they may suffer from moire artifacts, or beats, in cases where the scene has periodic patterns similar in frequency to the period of the CFA pattern. Non-periodic CFA patterns alleviate this problem. Also, fixed-pattern noise in CMOS sensors appears along columns of the sensor-array, and it is thus desirable to have a random or pseudo-random patterns of color filters for CFAs.

A number of CFA arrangements have appeared in the literature and been used commercially [4, 5, 6]. The periodic Bayer array [7] (Fig. 1(a)), first proposed in 1976, is by far the most popular CFA pattern. A notable feature of the Bayer array is that green is sampled at twice the density of red and blue since the luminance response of the human visual system (HVS) corresponds closely with the HVS response to the green range of the spectrum. Figure 1 shows a number of common periodic CFA arrangements.

The ability of any acquisition system to accurately reproduce color depends fundamentally on the sensitivity functions of the color filters. Much research has been directed at the problem of selection of spectral sensitivity functions in the case where multiple colors are acquired at a single location [8, 9, 10]. The selection of spectral sensitivity selection is all the more critical for CFA based acquisition systems, but the problem has received very little attention in the research community. In CFA based acquisition, in addition to the obvious effect on color reproduction, the spatial-chromatic sampling nature of CFA based schemes enforces a dependence of spatial or luminance reconstruction quality on the spectral sensitivity functions. Figure 2 shows typical spectral transmittance functions for RGB and CMY color filters.

Since the effective use of inter-band correlation is criti-

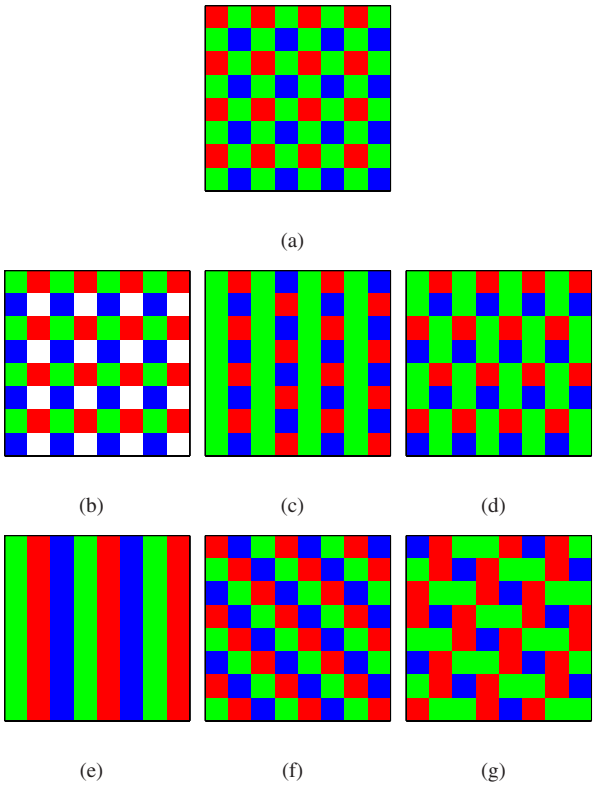

Figure 1. *Common periodic CFAs. (a) Bayer [7], (b) Gindele [6], (c) Yamanaka [4], (d) Lukac, (e) striped, (f) diagonal striped [3], (g) CFA pattern based on the Utah dot halftone (suggested by Charles M. Hains)*

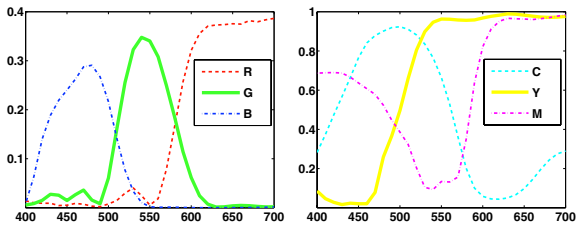

(a) RGB (b) CMY

Figure 2. *Spectral sensitivity functions. Ordinates represent transmittance, abscissae are wavelength in nm. (a),(b) RGB and CYM transmittances respectively from ImagEval's vCamera toolbox [11].*

cal to the performance of demosaicking algorithms (as seen in the survey by Gunturk *et al.* in [12]), color filter sensitivity functions that project incident radiance to a highly correlated sub-space appear desirable. But, a high inter-channel correlation has a detrimental effect on the discriminability of colors. Alleysson *et al.* [13] demonstrate this trade-off between color discrimination and spatial reconstruction quality.

In this paper we focus on the design of optimal spectral sensitivity functions for the periodic CFA patterns shown in Fig. 1. We use the optimal spectral sensitivity selection method proposed in [14]. Significantly, the optimization method is based on general image statistics and not on particular imaged scenes. A minimum MSE estimate of the image CIEXYZ tristimulus values is used to define an error criterion that incorporates both spatial and chromatic errors in a perceptually uniform color space. A constrained minimization of the criterion yields optimal values of the color filter sensitivity functions. Results are presented in the form of demosaicked images and s-CIELab error values. The proposed sensitivity functions perform significantly better than typical RGB and CMY filter transmittances both objectively and subjectively.

Image formation Model

In this section we summarize the modeling and optimization procedures detailed in [14]. Figure 3 depicts the image formation process for an image acquired at a spatial location in a sensor-array. Radiation from a light source is incident on a point in the scene with reflectance $x(\lambda)$. The reflected beam then travels through a color filter to an optical detector (CCD or CMOS device) that has a sensitivity $d(\lambda)$. The signal obtained at the detector is given by

$$c = \int_{\lambda_{min}}^{\lambda_{max}} f(\lambda)d(\lambda)x(\lambda)l(\lambda)d\lambda + \eta, \qquad (1)$$

where $l(\lambda)$ is the spectral power density of the illuminant, $f(\lambda)$ is the spectral transmittance of the color filter, and η is the measurement noise. The detector is sensitive in the wavelength range $(\lambda_{min}, \lambda_{max})$.

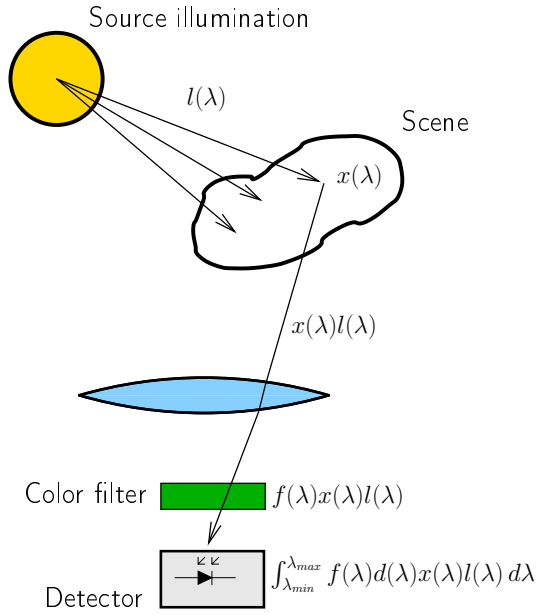

Figure 3. *Representation of the image formation process in color image acquisition with color filters*

In the discrete form (assuming that the visible spectrum is adequately sampled when sampled every 10nm in the range 400-700 nm), the image formation model may be expressed as

$$c = M^T Lx + \eta, \qquad (2)$$

where $x \in \mathbb{R}^{31\times 1}$ contains scene reflectance samples, $L \in \mathbb{R}^{31\times 31}$ is a diagonal matrix with samples of the radiant spectrum of the illuminant along its diagonal, and $M \in \mathbb{R}^{31\times 1}$ describes the combined filter-sensor response.

We extend (2) to describe the image formation model for an $m \times n$ sensor-array that samples p color channels at each pixel location. Let $f_i \in \mathbb{R}^{31\times 1}$, $i = 1,2,\cdots,p$, describe the sampled spectral sensitivity functions of the p colors and let $F = [f_1^T, f_2^T, \cdots, f_p^T]^T$. The image acquired at the sensor is described by the vector

$$y = \bar{F}\bar{L}x + \eta. \tag{3}$$

The scene is described by the vector of reflectance values $x = [x_1^T, x_2^T, \cdots, x_{mn}^T]^T$, where $x_i \in \mathbb{R}^{31\times 1}, 1 \le i \le mn$ are the sampled reflectance spectra acquired at the mn distinct pixel locations in the sensor array. The p-color image, $y \in \mathbb{R}^{pmn\times 1}$, is of the form $y = [y_1^T, y_2^T, \cdots, y_p^T]^S$, where $y_i \in \mathbb{R}^{mn\times 1}$ are the column-ordered color channels. The matrix $\bar{F}$ is constructed from f_i and $L_i \in \mathbb{R}^{31\times 31}$ is diagonal with sampled values of the illuminant spectrum as its diagonal elements. The matrix of illuminant spectra $\bar{L}$ in Eq. (3) is formed as $\bar{L} = \text{diag}(L_1, L_2, \cdots, L_{mn})$.

In CFA-based image acquisition, only one color is sampled at a particular location. The image formation model in this case is

$$g = Sy. \tag{4}$$

S is the sub-sampling matrix that reduces the pmn samples of y to the vector g of size $mn \times 1$ such that we are left with only one color sample at each pixel location.

The CIEXYZ space is the most commonly used device-independent color space in colorimetry [15]. Let $z = \bar{A}\bar{L}x$ be the column ordered representation of the scene in the CIE XYZ color space when viewed under the illuminant L. The matrix $\bar{A}$ is formed from the color matching functions $\bar{x}$, $\bar{y}$, and $\bar{z}$ that describe the CIEXYZ space.

We consider the noise-free case and assume wide sense stationary signals. The LMMSE estimate $\hat{z}$ of z with respect to g is given by

$$\hat{z} = R_{zg}R_{gg}^{-1}g, \tag{5}$$

where $R_{zg} = \mathrm{E}\{zg^T\}$, $R_{gg} = \mathrm{E}\{gg^T\}$. Substituting explicit expressions for R_{zg} and R_{gg} gives

$$\hat{z} = \left(\bar{A}\bar{L}R_{xx}\bar{L}^T\bar{F}^TS^T\right)\left(S\bar{F}\bar{L}R_{xx}\bar{L}^T\bar{F}^TS^T\right)^{-1}g. \tag{6}$$

The block matrix R_{xx} has the spectral autocorrelation matrices for each pixel location as its diagonal blocks, and has inter-pixel spectral crosscorrelation matrices as its off-diagonal blocks.

The XYZ tristimulus errors at each location of the array are arranged in a column-ordered form to form the error vector

$$e = z - \hat{z} = (\bar{A} - P)\bar{L}x, \tag{7}$$

where $P = \left(\bar{A}\bar{L}R_{xx}\bar{L}^T\bar{F}^TS^T\right)\left(S\bar{F}\bar{L}R_{xx}\bar{L}^T\bar{F}^TS^T\right)^{-1}S\bar{F}$.

Since errors in XYZ space do not reflect perceived differences in color, the error vector is transformed to the perceptually uniform linearized CIELab space. The error criterion is formed as as the expectation of the 2-norm of the aggregated CIELab errors at all spatial locations of the reconstructed p-color image and can be reduced to the form

$$\Delta E = \text{tr}\left(\bar{L}R_{xx}\bar{L}^T(\bar{A} - P)^T\bar{J}^T\bar{J}(\bar{A} - P)\right). \tag{8}$$

Figure 4 illustrates the formation of the error criterion, where $Y_yC_xC_z$ denotes the linearized CIELab space.

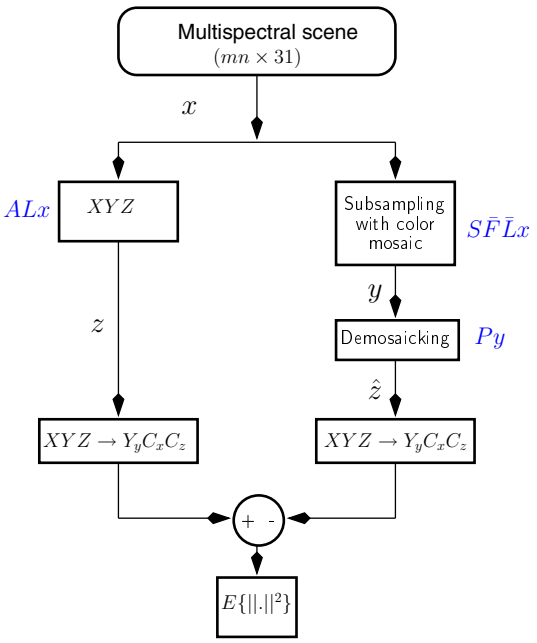

Figure 4. *The error criterion. All variables are as described in accompanying text.*

The criterion is revised to account for image acquisition under varying illuminants. Also, to ensure that the optimized filter sensitivities are reasonably smooth (to account for manufacturing limitations), a penalty on their roughness is included in the revised criterion:

$$\Phi = \Delta E_{D_{65}} + \Delta E_{D_{75}} + \Delta, E_{\text{uniform}} + \varepsilon. \tag{9}$$

where D_{65}, D_{75} and uniform are standard illuminants and ε is a cost on roughness.

Correlation matrix model

The correlation matrix R_{xx} is of the form

$$R_{xx} = \mathrm{E}\left\{\begin{bmatrix} x_1x_1^T & x_1x_2^T & \cdots & x_1x_{mn}^T \\ x_2x_1^T & x_2x_2^T & \cdots & x_2x_{mn}^T \\ \vdots & \vdots & \ddots & \vdots \\ x_{mn}x_1^T & x_{mn}x_2^T & \cdots & x_{mn}x_{mn}^T \end{bmatrix}\right\}$$
$$= \begin{bmatrix} R^{(1,1)} & R^{(1,2)} & \cdots & R^{(1,mn)} \\ R^{(2,1)} & R^{(2,2)} & \cdots & R^{(2,mn)} \\ \vdots & \vdots & \ddots & \vdots \\ R^{(mn,1)} & R^{(mn,2)} & \cdots & R^{(mn,mn)} \end{bmatrix}, \tag{10}$$

and contains elements due to the spectral correlation at a single spatial location and spatial correlations across the image. We will rely on a numerical optimization of (9) using Matlab's `fmincon` routine to arrive at an optimal value for F. The routine carries out a gradient-based search for the minimum and requires multiple computations of Φ and $\partial\Phi/\partial f_i$. This requires multiple products of large-dimension matrices of the type $\left(S\bar{F}\bar{L}R_{xx}\bar{L}^T\bar{F}^TS^T\right)$ seen in (6). The challenge in modeling a generalized R_{xx} applicable for all acquired scenes lies in forming blocks of R_{xx} that give it a regular structure that lends itself to optimized computation while not defying the statistical properties of any particular scene.

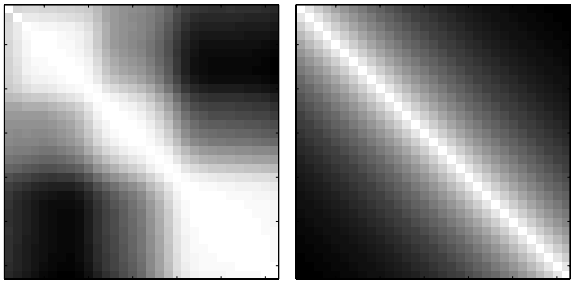

(a) Super-image (b) Proposed model

Figure 5. *The spectral correlation matrix $R^{(1,1)}$ for (a) the super-image obtained by accumulating spectral data from all the images in [16] (b) for the proposed model.*

Here, we make the following assumptions in forming R_{xx}:

1. The spectral correlation at a particular spatial location is separable from the spatial correlation in samples across the acquired image in a particular wavelength band.
2. The correlation coefficients that form the elements of $R^{(k,k)}$ (10) are an exponential function of wavelength separation.
3. The correlation matrices $R^{(k,l)}$, that incorporate spatial correlations in the image bands are an exponential function of spatial distance.
4. The acquired image is spatially periodic. This yields an R_{xx} that is block-circulant with block-circulant Toeplitz blocks.

Please see [14] for more details on the form of R_{xx}. Hordley *et al.* [16] have provided a database of multi-spectral images captured using a Spectracube© camera. These spectral images were acquired under controlled conditions under the D_{75} illuminant. A correction for the illuminant was applied to arrive at reflectance values sampled every 10 nm in the range 400–700 nm. Figure 5 shows representations of $R^{(1,1)}$ for the proposed model by considering all the multispectral images in [16].

Experiments

We use the proposed framework to obtain optimal color filter transmittance functions for the CFA patterns in Fig. 1. A constrained minimization of the criterion in (9) is carried out to arrive at optimal estimates for the filter sensitivities represented by f_i for each CFA pattern. The constraints are that $f_i \in (0,1)$. Since a global minimum is not assured, we generate a number of distinct initial conditions and choose the least value of the criterion to arrive at the filter sensitivities f_i. Initial values of f_i are assumed to be Gaussian curves in the wavelength domain and are given by

$$f_i(\lambda) = e^{-\frac{(\lambda-\mu_i)^2}{\sigma_i^2}}. \tag{11}$$

An initial condition is defined by the vectors $\mu = [\mu_1, \mu_2, \cdots, \mu_p]^T$ and $\sigma = [\sigma_1, \sigma_2, \cdots, \sigma_p]^T$ which contain the means and standard deviations respectively of the p Gaussian curves that represent the filter sensitivities. The elements of μ and σ are uniform random variables defined over the visible spectrum with the following constraints: $400 \leq \mu_i \leq 700$ and $\rho \leq \sigma_i \leq 10\rho$, where $\rho = 30$. The optimal filter sensitivities obtained for CFA pattern in Fig. 1 are shown in Fig. 6.

We used the database of multispectral images [16] for our experiments. The simulation pipeline shown in Fig. 7 was used to arrive at demosaicked images from the available multispectral images and for later objective and subjective comparisons. For comparison of spectral sensitivity functions, we used typical RGB and CMY filter sensitivities from ImagEval's vCamera MATLAB toolbox [11](Fig. 2).

Since the object here is to compare the performance of color filter sensitivity functions, we used the linear MMSE estimator in (6) for demosaicking even though many sophisticated demosaicking algorithms are known. The s-CIELab error metric was used to quantify the error between the original image as obtained from the XYZ values of the multispectral images and the corresponding demosaicked images. Average s-CIELab ΔE values of all images from the multispectral image database for each of the CFA patterns in Fig. 1 as acquired with the RGB, CMY, and the optimized sensitivities are given in Table 1. Evidently, the optimized color filters perform significantly better than the standard RGB and CMY filters.

Table 1: Average s-CIELab ΔE values. All images in [16] are sampled according to the patterns in Fig. 1 and the demosaicked results are compared with the original multispectral scene as shown in Fig. 7.

Pattern	ΔE_S RGB	ΔE_S CMY	ΔE_S optimal
(a)	6.0911	5.9310	**3.2724**
(b)	6.5438	5.8246	**3.9508**
(c)	6.5051	6.6076	**3.9725**
(d)	6.2251	6.3891	**3.3761**
(e)	7.3646	8.4028	**5.1840**
(f)	6.3924	6.3206	**3.2203**
(g)	6.6039	6.7034	**3.6788**

Figure 8 shows results of a subjective comparison for an image cropped from image 3 of the database. The rows of Figure 8 show results of demosaicking of images sampled with the CFA patterns in Fig. 1. On each row, for a particular CFA pattern, demosaicking results of images sampled with RGB, CMY, and optimized filter sensitivities appear from left to right respectively. Figure 8 also shows the s-CIELab ΔE error images

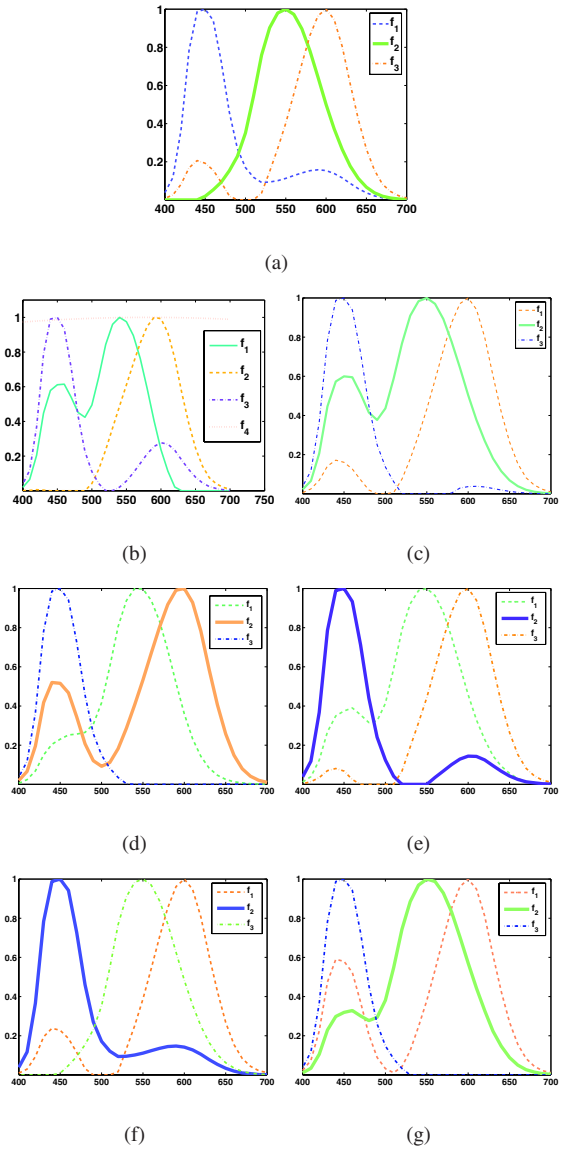

Figure 6. *(a)-(g) Optimal spectral sensitivity functions obtained for the CFA patterns shown in Figs. 1(a)-1(g) respectively. Ordinates represent normalized transmittances. Bolder lines correspond to the optimal sensitivities obtained at the location of the green filter in the respective CFA patterns.*

corresponding to each reconstructed image. The images obtained by sampling with optimized sensitivity functions show fewer luminance (most apparent at the edges) and chrominance (manifest as hue-shifts in the smooth regions) artifacts.

Conclusions

In this paper we have presented optimal color filter spectral sensitivity functions for several periodic CFA patterns. For the optimization, we use a framework that is based on a unified spatial-chromatic sampling model and is not dependent on particular images, but on general image statistics. The results of simulations reflect the significant role played by color filter

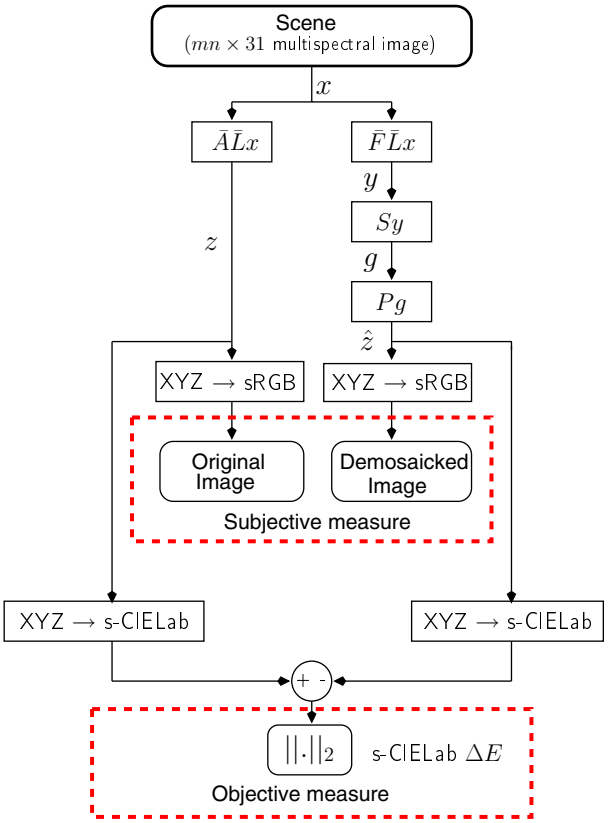

Figure 7. *The simulation pipeline. All variables are as described in preceding sections*

transmittances in the quality of demosaicking. Our framework also allows for a comparison of the CFA patterns considered. Our results suggest that from the point of view of optimal linear mininmum MSE reconstruction, the diagonal striped array in Fig. 1(g) performs best, and the striped CFA (Fig. 1(e)) performs worst. Optimized color filter sensitivities consistently yield results significantly superior to results obtained from typical RGB and CMY filters in terms of both the s-CIELab ΔE metric, and subjectively, as seen in reconstructed images.

References

[1] K. Parulski and K.E. Spaulding, "Color image processing for digital cameras," in *Digital Color Imaging Handbook*, Gaurav Sharma, Ed., pp. 728–757. CRC Press, Inc., Boca Raton, FL, USA, 2002.

[2] J. Adams, K. Parulski, and K. Spaulding, "Color processing in digital cameras," *IEEE Micro*, vol. 18, no. 4, pp. 20–30, Nov/Dec 1998.

[3] R. Lukac and K.N. Plataniotis, "Color filter arrays: Design and performance analysis," *IEEE Transactions on Consumer Electronics*, vol. 51, no. 4, pp. 1260–1267, Nov. 2005.

[4] S. Yamanaka, "Solid state camera," U.S. Patent 4054906, 1977.

[5] Manu Parmar and Stanley J. Reeves, " A perceptually based design methodology for color filter arrays ," *Acoustics, Speech, and Signal Processing, 2004. Proceedings. (ICASSP '04). IEEE International Conference on*, vol.

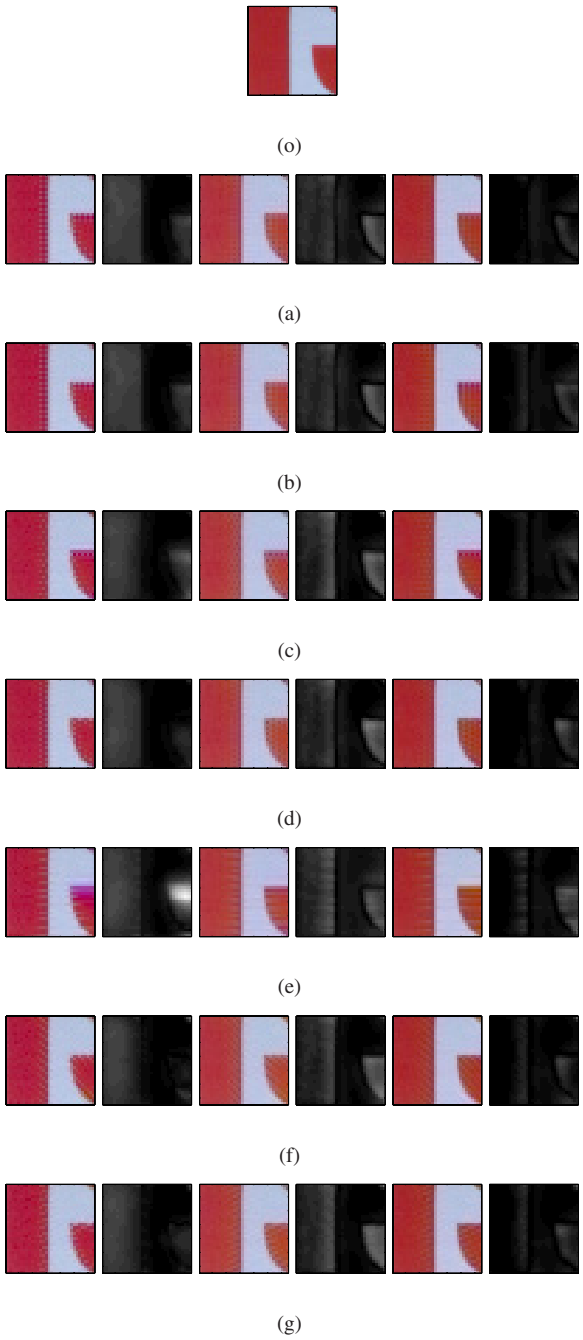

Figure 8. *sRGB representations (for the D_{65} illuminant) of an image cropped from image 3 from the database of multispectral images [16]. (o) Original image. (a)-(g) From left to right — Images reconstructed from the CFA sampled images obtained from the RGB, CMY, and optimized color filters respectively. s-CIELab ΔE error images appear to the right of each reconstructed image.*

53, pp. 473–476., 2004.

[6] E.B. Gindele and A.C. Gallagher, "Sparsely sampled image sensing device with color and luminance photosites," U.S. Patent 6476865 B1, Nov. 2002.

[7] B.E. Bayer, "Color imaging array," U.S. Patent 3971065, July 1976.

[8] Michael J. Vrhel and H. Joel Trussell, "Color filter selection for color correction in the presence of noise," in *IEEE International Conference on Acoustics, Speech, and Signal Processing*, 1993, pp. 313–316.

[9] M. Wolski, C. Bouman, J.P. Allebach, and E. Walowit, "Optimization of sensor response functions for colorimetry of reflective and emissive objects," *IEEE Trans. Image Processing*, vol. 5, no. 3, pp. 507–517, Mar 1996.

[10] P.L. Vora and H.J. Trussell, "Mathematical methods for the design of color scanning filters," *IEEE Trans. Image Processing*, vol. 6, no. 2, pp. 312–320, Feb 1997.

[11] J. E. Farrell, F. Xiao, P. B. Catrysse, and B. A. Wandell, "A simulation tool for evaluating digital camera image quality," in *Proceedings of IS&T/SPIEs Electronic Imaging 2004: Image Quality and System Performance*, Jan. 2004, vol. 5294.

[12] B.K. Gunturk, Y. Glotzbach, Y. Altunbasak, R.W. Schafer, and R. Mersereau, "Demosaicking: Color filter array interpolation in single chip digital cameras," *IEEE Signal Processing Mag.*, vol. 22, no. 1, pp. 44–54, Jan. 2005.

[13] David Alleysson, Sabine Süsstrunk, and Joanna Marguier, "Influence of spectral sensitivity functions on color demosaicing," *Proceedings of the eleventh Color Imaging Conference: Color Science and Engineering Systems, Technologies, Applications*, pp. 351–357, November 2003.

[14] Manu Parmar and Stanley J. Reeves, "Selection of optimal spectral sensitivity functions for color filter arrays," *International Conference on Image Processing, 2006, Proceedings of; to appear*, 2006.

[15] Gaurav Sharma, Ed., *Digital Color Imaging Handbook*, chapter one: Color fundamentals for digital imaging, CRC Press, Inc., Boca Raton, FL, USA, 2002.

[16] Steven D. Hordley, Graham D. Finlayson, and Peter Morovic, "A multi-spectral image database and an application to image rendering across illumination," in *Proceedings of Third International Conference on Image and Graphics, Hong-Kong China,*, December 2004, pp. 349–355.

Author Biography

Manu Parmar *received the B.E. degree in electrical engineering from the Government College of Engineering, Pune, India, and the M.S. degree in electrical engineering from Auburn University, Auburn, AL, in 2000 and 2002 respectively. He is currently a Ph.D. candidate in the Dept. of Electrical & Computer Engineering at Auburn University. His research interests include signal and image processing, image restoration, and color image processing. He is a member of the IEEE and IS&T.*

Stanley J. Reeves *received the PhD in 1990 from the Georgia Institute of Technology. He is a professor in the Department of Electrical and Computer Engineering at Auburn University. He serves as an associate editor for IEEE Transactions on Image Processing. His interests include image restoration and reconstruction, optimal image acquisition, and magnetic resonance imaging.*